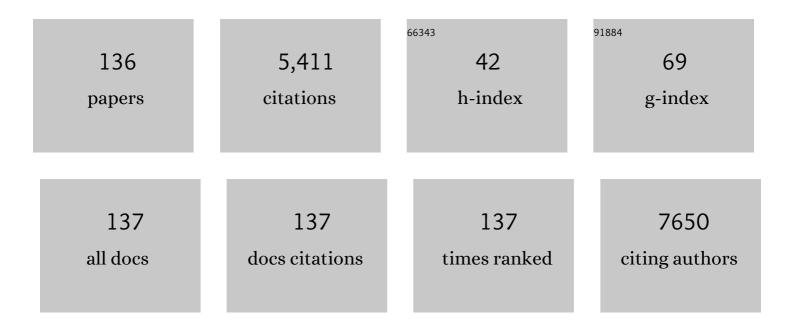
List of Publications by Year in descending order

Source: https://exaly.com/author-pdf/4964030/publications.pdf Version: 2024-02-01



YANG HANG

#	Article	IF	CITATIONS
1	Surface Ligand Engineering for Near-Unity Quantum Yield Inorganic Halide Perovskite QDs and High-Performance QLEDs. Chemistry of Materials, 2018, 30, 6099-6107.	6.7	217
2	Shape and phase evolution from CsPbBr <sub>3</sub> perovskite nanocubes to tetragonal CsPb <sub>2</sub> Br <sub>5</sub> nanosheets with an indirect bandgap. Chemical Communications, 2016, 52, 11296-11299.	4.1	210
3	Fabrication of Ultrathin Bi <sub>2</sub> S <sub>3</sub> Nanosheets for Highâ€Performance, Flexible, Visible–NIR Photodetectors. Small, 2015, 11, 2848-2855.	10.0	205
4	In Situ Fabrication of Vertical Multilayered MoS <sub>2</sub> /Si Homotype Heterojunction for High-Speed Visible-Near-Infrared Photodetectors. Small, 2016, 12, 1062-1071.	10.0	185
5	Phase transition induced recrystallization and low surface potential barrier leading to 10.91%-efficient CsPbBr3 perovskite solar cells. Nano Energy, 2019, 65, 104015.	16.0	170
6	Sodium storage and transport properties in pyrolysis synthesized MoSe 2 nanoplates for high performance sodium-ion batteries. Journal of Power Sources, 2015, 283, 187-194.	7.8	159
7	Glucose-assisted synthesis of Na3V2(PO4)3/C composite as an electrode material for high-performance sodium-ion batteries. Journal of Power Sources, 2014, 265, 325-334.	7.8	157
8	Ultrafast kinetics net electrode assembled via MoSe2/MXene heterojunction for high-performance sodium-ion batteries. Chemical Engineering Journal, 2020, 385, 123839.	12.7	141
9	Dualâ€Phase CsPbBr <sub>3</sub> –CsPb <sub>2</sub> Br <sub>5</sub> Perovskite Thin Films via Vapor Deposition for Highâ€Performance Rigid and Flexible Photodetectors. Small, 2018, 14, 1702523.	10.0	139
10	Accelerating hole extraction by inserting 2D Ti <sub>3</sub> C <sub>2</sub> -MXene interlayer to all inorganic perovskite solar cells with long-term stability. Journal of Materials Chemistry A, 2019, 7, 20597-20603.	10.3	130
11	Solventâ€Polarityâ€Engineered Controllable Synthesis of Highly Fluorescent Cesium Lead Halide Perovskite Quantum Dots and Their Use in White Lightâ€Emitting Diodes. Advanced Functional Materials, 2016, 26, 8478-8486.	14.9	129
12	Phase Transition Mechanism and Electrochemical Properties of Nanocrystalline MoSe <sub>2</sub> as Anode Materials for the High Performance Lithium-Ion Battery. Journal of Physical Chemistry C, 2015, 119, 10197-10205.	3.1	122
13	Interface engineering using a perovskite derivative phase for efficient and stable CsPbBr <sub>3</sub> solar cells. Journal of Materials Chemistry A, 2018, 6, 14255-14261.	10.3	117
14	Efficient CsPbBr <sub>3</sub> Perovskite Lightâ€Emitting Diodes Enabled by Synergetic Morphology Control. Advanced Optical Materials, 2019, 7, 1801534.	7.3	117
15	Self-powered and fast-speed photodetectors based on CdS:Ga nanoribbon/Au Schottky diodes. Journal of Materials Chemistry, 2012, 22, 23272.	6.7	116
16	Charge deformation and orbital hybridization: intrinsic mechanisms on tunable chromaticity of Y3Al5O12:Ce3+ luminescence by doping Gd3+ for warm white LEDs. Scientific Reports, 2015, 5, 11514.	3.3	102
17	Device structure-dependent field-effect and photoresponse performances of p-type ZnTe:Sb nanoribbons. Journal of Materials Chemistry, 2012, 22, 6206.	6.7	96
18	Largeâ€Area Lasing and Multicolor Perovskite Quantum Dot Patterns. Advanced Optical Materials, 2018, 6, 1800474.	7.3	95

#	Article	IF	CITATIONS
19	Graphitic C3N4 quantum dots for next-generation QLED displays. Materials Today, 2019, 22, 76-84.	14.2	85
20	Self-combustion synthesis of Na3V2(PO4)3 nanoparticles coated with carbon shell as cathode materials for sodium-ion batteries. Electrochimica Acta, 2015, 155, 23-28.	5.2	84
21	Long Cycle Life, Low Selfâ€Discharge Sodium–Selenium Batteries with High Selenium Loading and Suppressed Polyselenide Shuttling. Advanced Energy Materials, 2018, 8, 1701953.	19.5	84
22	Enhancing Hybrid Perovskite Detectability in the Deep Ultraviolet Region with Down-Conversion Dual-Phase (CsPbBr <sub>3</sub> –Cs <sub>4</sub> PbBr <sub>6</sub> ) Films. Journal of Physical Chemistry Letters, 2018, 9, 1592-1599.	4.6	82
23	All-Inorganic Perovskite Nanocrystals with a Stellar Set of Stabilities and Their Use in White Light-Emitting Diodes. ACS Applied Materials & Interfaces, 2018, 10, 37267-37276.	8.0	82
24	Crystallographic-plane tuned Prussian-blue wrapped with RGO: a high-capacity, long-life cathode for sodium-ion batteries. Journal of Materials Chemistry A, 2017, 5, 3569-3577.	10.3	75
25	Mixed cation perovskite solar cells by stack-sequence chemical vapor deposition with self-passivation and gradient absorption layer. Nano Energy, 2018, 48, 536-542.	16.0	70
26	High Efficient Hole Extraction and Stable Allâ€Bromide Inorganic Perovskite Solar Cells via Derivativeâ€Phase Gradient Bandgap Architecture. Solar Rrl, 2019, 3, 1900030.	5.8	67
27	High-gain visible-blind UV photodetectors based on chlorine-doped n-type ZnS nanoribbons with tunable optoelectronic properties. Journal of Materials Chemistry, 2011, 21, 12632.	6.7	64
28	Deep red phosphors SrAl <sub>12</sub> O <sub>19</sub> :Mn <sup>4+</sup> ,M (M = Li <sup>+</sup> ,) Status Solidi (A) Applications and Materials Science, 2013, 210, 1433-1437.	Tj ETQq0 1.8	0 0 rgBT /Ov 59
29	Understanding the Local and Electronic Structures toward Enhanced Thermal Stable Luminescence of CaAlSiN <sub>3</sub> :Eu <sup>2+</sup> . Chemistry of Materials, 2016, 28, 5505-5515.	6.7	57
30	Rapid, stable and self-powered perovskite detectors via a fast chemical vapor deposition process. RSC Advances, 2017, 7, 18224-18230.	3.6	57
31	Dimensional Gradient Structure of CoSe2@CNTs–MXene Anode Assisted by Ether for High-Capacity, Stable Sodium Storage. Nano-Micro Letters, 2021, 13, 40.	27.0	54
32	Reduced Graphene Oxide-Anchored Manganese Hexacyanoferrate with Low Interstitial H <sub>2</sub> O for Superior Sodium-Ion Batteries. ACS Applied Materials & Interfaces, 2018, 10, 34222-34229.	8.0	53
33	Poly(3,4-ethylenedioxythiophene)/MoS <sub>2</sub> nanocomposites with enhanced electrochemical capacitance performance. RSC Advances, 2014, 4, 56926-56932.	3.6	52
34	Enhanced p-Type Conductivity of ZnTe Nanoribbons by Nitrogen Doping. Journal of Physical Chemistry C, 2010, 114, 7980-7985.	3.1	51
35	3D Ag@C Cloth for Stable Anode Free Sodium Metal Batteries. Small Methods, 2021, 5, e2001050.	8.6	51
36	High Quality MoSe <sub>2</sub> Nanospheres with Superior Electrochemical Properties for Sodium Batteries. Journal of the Electrochemical Society, 2016, 163, A1627-A1632.	2.9	49

#	Article	IF	CITATIONS
37	Cadmium-doped flexible perovskite solar cells with a low-cost and low-temperature-processed CdS electron transport layer. RSC Advances, 2017, 7, 19457-19463.	3.6	48
38	Highly bright and low turn-on voltage CsPbBr3 quantum dot LEDs via conjugation molecular ligand exchange. Nano Research, 2019, 12, 109-114.	10.4	48
39	Luminescent properties of La2LiTaO6:Mn4+ and its application as red emission LEDs phosphor. Applied Physics A: Materials Science and Processing, 2014, 117, 1777-1783.	2.3	45
40	A novel carbon-decorated hollow flower-like MoS2 nanostructure wrapped with RGO for enhanced sodium-ion storage. Chemical Engineering Journal, 2018, 343, 180-188.	12.7	44
41	Carbon electrode engineering for high efficiency all-inorganic perovskite solar cells. RSC Advances, 2020, 10, 12298-12303.	3.6	44
42	Design and construction of ultra-thin MoSe2 nanosheet-based heterojunction for high-speed and low-noise photodetection. Nano Research, 2016, 9, 2641-2651.	10.4	43
43	High quantum-yield CdSe <sub><i>x</i></sub> S <sub>1â^'<i>x</i></sub> /ZnS core/shell quantum dots for warm white light-emitting diodes with good color rendering. Nanotechnology, 2013, 24, 285201.	2.6	42
44	Full-spectra hyperfluorescence cesium lead halide perovskite nanocrystals obtained by efficient halogen anion exchange using zinc halogenide salts. CrystEngComm, 2017, 19, 1165-1171.	2.6	42
45	High-performance CdS:P nanoribbon field-effect transistors constructed with high-κ dielectric and top-gate geometry. Applied Physics Letters, 2010, 96, .	3.3	41
46	N-doped Fe3C@C as an efficient polyselenide reservoir for high-performance sodium-selenium batteries. Energy Storage Materials, 2019, 16, 374-382.	18.0	41
47	Construction of high-quality CdS:Ga nanoribbon/silicon heterojunctions and their nano-optoelectronic applications. Nanotechnology, 2011, 22, 405201.	2.6	40
48	Preparation of highly luminescent BaSO <sub>4</sub> protected CdTe quantum dots as conversion materials for excellent color-rendering white LEDs. Journal of Materials Chemistry C, 2015, 3, 2831-2836.	5.5	36
49	Solution assembly MoS <sub>2</sub> nanopetals/GaAs n–n homotype heterojunction with ultrafast and low noise photoresponse using graphene as carrier collector. Journal of Materials Chemistry C, 2017, 5, 140-148.	5.5	36
50	Electrochemically Stable Sodium Metalâ€Tellurium/Carbon Nanorods Batteries. Advanced Energy Materials, 2019, 9, 1903046.	19.5	33
51	Graphite cluster/copper-based powder metallurgy composite for pantograph slider with well-behaved mechanical and wear performance. Powder Technology, 2019, 344, 551-560.	4.2	33
52	Photoluminescence properties of Eu3+ and Bi3+ in YBO3 host under vacuum ultraviolet/ultraviolet excitation. Journal of Applied Physics, 2009, 105, 013513.	2.5	31
53	A water–ethanol phase assisted co-precipitation approach toward high quality quantum dot–inorganic salt composites and their application for WLEDs. Green Chemistry, 2015, 17, 4439-4445.	9.0	31
54	Surface-activation modified perovskite crystallization for improving photovoltaic performance. Materials Today Energy, 2017, 5, 173-180.	4.7	31

#	Article	IF	CITATIONS
55	Lead-Free Perovskite Narrow-Bandgap Oxide Semiconductors of Rare-Earth Manganates. ACS Omega, 2020, 5, 8766-8776.	3.5	31
56	Mechanical and wear performances of aluminum/sintered-carbon composites produced by pressure infiltration for pantograph sliders. Powder Technology, 2018, 326, 54-61.	4.2	30
57	High-performance photodetectors and enhanced field-emission of CdS nanowire arrays on CdSe single-crystalline sheets. Journal of Materials Chemistry C, 2014, 2, 8252-8258.	5.5	28
58	N-doped carbon dots from phenol derivatives for excellent colour rendering WLEDs. RSC Advances, 2018, 8, 4850-4856.	3.6	28
59	High-speed ultraviolet-visible-near infrared photodiodes based on p-ZnS nanoribbon–n-silicon heterojunction. CrystEngComm, 2013, 15, 1635.	2.6	27
60	Self-Combustion Synthesis and Ion Diffusion Performance of NaV <sub>6</sub> O <sub>15</sub> Nanoplates as Cathode Materials for Sodium-Ion Batteries. Journal of the Electrochemical Society, 2015, 162, A697-A703.	2.9	25
61	Direct photodissociation of toluene molecules to photoluminescent carbon dots under pulsed laser irradiation. Carbon, 2016, 105, 416-423.	10.3	25
62	Ca <sub>3 â^' <i>x</i></sub> Bi <sub><i>x</i></sub> Co <sub>4</sub> O <sub>9</sub> and Ca <sub>1 â^' <i>y</i></sub> Sm <sub><i>y</i></sub> MnO <sub>3</sub> thermoelectric materials and powerâ€generation devices. Physica Status Solidi (A) Applications and Materials Science, 2011, 208, 147-155.	their 1.8	24
63	Cu2ZnSnS4 and Cu2ZnSn(S1â^'xSex)4 nanocrystals: room-temperature synthesis and efficient photoelectrochemical water splitting. Journal of Materials Chemistry A, 2017, 5, 25230-25236.	10.3	24
64	White-light-emitting CdSe quantum dots with "magic size―via one-pot synthesis approach. Physica Status Solidi (A) Applications and Materials Science, 2010, 207, 2472-2477.	1.8	21
65	PbS Quantum-Dot Depleted Heterojunction Solar Cells Employing CdS Nanorod Arrays as the Electron Acceptor with Enhanced Efficiency. ACS Applied Materials & Interfaces, 2015, 7, 23117-23123.	8.0	20
66	Nearâ€Infrared Photoactive Semiconductor Quantum Dots for Solar Cells. Advanced Energy Materials, 2021, 11, 2101923.	19.5	20
67	Structure and electrical properties of p-type twin ZnTe nanowires. Applied Physics A: Materials Science and Processing, 2011, 102, 469-475.	2.3	19
68	Ultralow-voltage and high gain photoconductor based on ZnS:Ga nanoribbons for the detection of low-intensity ultraviolet light. Journal of Materials Chemistry C, 2014, 2, 3583.	5.5	19
69	Microstructure and Current Carrying Wear Behaviors of Copper/Sintered–Carbon Composites for Pantograph Sliders. Metals and Materials International, 2021, 27, 3398-3408.	3.4	19
70	Ammonium hydroxide modulated synthesis of high-quality fluorescent carbon dots for white LEDs with excellent color rendering properties. Nanotechnology, 2016, 27, 295202.	2.6	18
71	Three-dimensional architecture hybrid perovskite solar cells using CdS nanorod arrays as an electron transport layer. Nanotechnology, 2018, 29, 025401.	2.6	18
72	Fabrication of a Sandwiched Core Carbon Sphere@Na <sub>3</sub> V <sub>2</sub> (PO <sub>4</sub> ) <sub>2</sub> O <sub>2</sub> F@N-Doped Carbon Cathode for Superior Sodium-Ion Batteries. ACS Applied Energy Materials, 2021, 4, 3952-3961.	5.1	18

YANG JIANG

#	Article	IF	CITATIONS
73	Inverted quantum-dot solar cells with depleted heterojunction structure employing CdS as the electron acceptor. Solar Energy Materials and Solar Cells, 2015, 137, 287-292.	6.2	17
74	PVP-modulated synthesis of NaV6O15 nanorods as cathode materials for high-capacity sodium-ion batteries. Journal of Materials Science, 2016, 51, 8986-8994.	3.7	17
75	The temperatureâ€sensitive luminescence of (Y,Gd)VO <sub>4</sub> :Bi <sup>3+</sup> ,Eu <sup>3+</sup> and its application for stealth antiâ€counterfeiting. Physica Status Solidi - Rapid Research Letters, 2012, 6, 321-323.	2.4	16
76	The red luminescence of Sr4 Al14 O25 :Mn4+ enhanced by coupling with the SrAl2 O4 phase in the 3SrO · 5Al2 O3 system. Physica Status Solidi (A) Applications and Materials Science, 2013, 210, 1791-3	1798.	16
77	Construction of crossed heterojunctions from p-ZnTe and n-CdSe nanoribbons and their photoresponse properties. Journal of Materials Chemistry C, 2014, 2, 6547.	5.5	16
78	Ultrasensitive PbSâ€Quantumâ€Dot Photodetectors for Visible–Nearâ€Infrared Light Through Surface Atomicâ€Ligand Exchange. Particle and Particle Systems Characterization, 2015, 32, 1102-1109.	2.3	16
79	Direct deposition of Sn-doped CsPbBr <sub>3</sub> perovskite for efficient solar cell application. RSC Advances, 2021, 11, 3380-3389.	3.6	16
80	Self-ignition route to Ag-doped Na1.7Co2O4 and its thermoelectric properties. Journal of Alloys and Compounds, 2009, 467, 444-449.	5.5	15
81	Green chemical approaches to ZnSe quantum dots: preparation, characterisation and formation mechanism. Journal of Experimental Nanoscience, 2010, 5, 106-117.	2.4	15
82	Oneâ€pot synthesis of homogeneous CdSe <sub><i>x</i></sub> S <sub>1â^'<i>x</i></sub> alloyed quantum dots with tunable composition in a green Nâ€oleoylmorpholine solvent. Physica Status Solidi (A) Applications and Materials Science, 2012, 209, 306-312.	1.8	15
83	Full visible waveband tunable formamidinium halides hybrid perovskite QDs via anion-exchange route and their high luminous efficiency LEDs. Journal of Alloys and Compounds, 2019, 791, 814-821.	5.5	15
84	Inverse Fabrication of Li <sub>2</sub> Sâ€Nanocrystals@Dopedâ€Carbon Loaded on Woven Carbon Fibers to Spatial Structure Cathodes for Highâ€Stable Lithium–Sulfur Batteries. Small Methods, 2020, 4, 2000463.	8.6	14
85	Fine-tuning the crystal structure of CdSe quantum dots by varying the dynamic characteristics of primary alkylamine ligands. CrystEngComm, 2018, 20, 4492-4498.	2.6	13
86	Microstructure and properties of Al-60wt.%Si composites prepared by powder semi-solid squeeze. Powder Technology, 2019, 343, 95-100.	4.2	13
87	Synthesis of NbSe <sub>2</sub> single-crystalline nanosheet arrays for UV photodetectors. CrystEngComm, 2020, 22, 5710-5715.	2.6	13
88	Magnificent CdS three-dimensional nanostructure arrays: the synthesis of a novel nanostructure family for nanotechnology. CrystEngComm, 2011, 13, 145-152.	2.6	12
89	High performance visible–near-infrared PbS-quantum-dots/indium Schottky diodes for photodetectors. Nanotechnology, 2017, 28, 055202.	2.6	12
90	Hybrid perovskite exchange of PbS quantum dots for fast and high-detectivity visible–near-infrared photodetectors. Journal of Materials Chemistry C, 2020, 8, 7812-7819.	5.5	12

#	Article	IF	CITATIONS
91	A Ni-doping-induced phase transition and electron evolution in cobalt hexacyanoferrate as a stable cathode for sodium-ion batteries. Physical Chemistry Chemical Physics, 2021, 23, 2491-2499.	2.8	12
92	Formation of the amorphous phase in the carbothermal reduction and nitridation route to SrSi <sub>2</sub> O <sub>2</sub> N <sub>2</sub> : Eu <sup>2+</sup> : a new understanding of the catalytic effect of carbon in the synthesis of Sr <sub>2</sub> Si <sub>5</sub> N <sub>8</sub> : Eu <sup>2+</sup> for white LEDs. RSC Advances, 201 44317-44321.	3.6 4, 4,	11
93	High luminescent aqueous CdZnTe QDs incorporated in CaCO 3 for excellent color-rendering WLEDs. Journal of Alloys and Compounds, 2017, 712, 543-548.	5.5	11
94	Porous BN Nanofibers Enable Long ycling Life Sodium Metal Batteries. Small, 2020, 16, e2002671.	10.0	11
95	Electron oriented injection TiSe <sub>2</sub> –C laminated heterojunctions derived from terminal functionalized MXene for high-rate sodium ion storage. Journal of Materials Chemistry A, 2021, 9, 27684-27691.	10.3	11
96	Fabricating Na/In/C Composite Anode with Natrophilic Na–In Alloy Enables Superior Na Ion Deposition in the EC/PC Electrolyte. Nano-Micro Letters, 2022, 14, 23.	27.0	11
97	Auto-ignition route to thermoelectric oxide NaxCo2O4 powder with high compactibility. Powder Technology, 2008, 184, 25-30.	4.2	10
98	Large conductance switching nonvolatile memories based on p-ZnS nanoribbon/n-Si heterojunction. Journal of Materials Chemistry C, 2013, 1, 1238-1244.	5.5	10
99	Dataset of emission and excitation spectra, UV–vis absorption spectra, and XPS spectra of graphitic C3N4. Data in Brief, 2018, 21, 501-510.	1.0	10
100	Synthesis and spectrum stability of high quality CdTe quantum dots capped with stearate groups in N-oleoylmorpholine solvent. Journal of Crystal Growth, 2010, 312, 2656-2660.	1.5	9
101	Hybrid Colloidal Stabilization Mechanism toward Improved Photoluminescence and Stability of CdSe/CdS Core/Shell Quantum Dots. Langmuir, 2017, 33, 7124-7129.	3.5	9
102	Highly efficient and blue-emitting CsPbBr <sub>3</sub> quantum dots synthesized by two-step supersaturated recrystallization. Nanotechnology, 2021, 32, 145712.	2.6	9
103	Ultralow Contact Resistivity of Cu/Au With \$p\$-Type ZnS Nanoribbons for Nanoelectronic Applications. IEEE Electron Device Letters, 2013, 34, 810-812.	3.9	8
104	lon- and air-tailored micro-honeycomb structures for superior Na-ion storage in coir-derived hard carbon. New Journal of Chemistry, 2019, 43, 10449-10457.	2.8	8
105	Independent dispersed and highly water-oxygen environment stable FAPbBr3 QDs-polymer composite for down-conversion display films. Chemical Engineering Journal, 2022, 428, 130974.	12.7	8
106	Co-Vacancy, Co <sub>1â^'x</sub> S@C flower-like nanosheets derived from MOFs for high current density cycle performance and stable sodium-ion storage. New Journal of Chemistry, 2021, 45, 6865-6871.	2.8	7
107	Suppressing ion migration of CsPbBr <sub>x</sub> I <sub>3-x </sub> nanocrystals by Nickel doping and the application in high-efficiency WLEDs. Nanotechnology, 2021, 32, 335601.	2.6	7
108	Hybrid Perovskite Photoconductivity Visible Region Detector with High Speed and Stability. Nano, 2017, 12, 1750150.	1.0	6

#	Article	IF	CITATIONS
109	Nitrogen-rich hierarchical porous carbon materials with interconnected channels for high stability supercapacitors. New Journal of Chemistry, 2019, 43, 1864-1873.	2.8	6
110	Interface Engineering of a Sandwich Flexible Electrode PAn@CoHCF Rooted in Carbon Cloth for Enhanced Sodium-Ion Storage. ACS Applied Materials & (), 11, 2021, 13, 23794-23802.	8.0	6
111	Effect of flake graphite content on wear between behavior between P/M copper-based pantograph slide and contact wire. Materials Research Express, 2020, 7, 076510.	1.6	6
112	Thermoelectric properties of rapid hot pressed polycrystalline Ag <sub>1â^'<i>x</i></sub> Pb <sub>18</sub> SbTe <sub>20</sub> synthesized from doping PbTe nanocrystals. Physica Status Solidi (A) Applications and Materials Science, 2010, 207, 163-169.	1.8	5
113	A Na-Rich Nanocomposite of Na1.83Ni0.12Mn0.88Fe(CN) <sub>6</sub> /RGO as Cathode for Superior Performance Sodium-Ion Batteries. Nano, 2018, 13, 1850064.	1.0	5
114	Size-Dependent Plasmonic Mode Evolution and SERS Performance of Î <sup>2</sup> -Sn Nanoparticles. Journal of Physical Chemistry C, 2019, 123, 735-738.	3.1	5
115	Self-doped 3-hexylthiophene-b-sodium styrene sulfonate block copolymer: synthesis and its organization with CdSe quantum dots. RSC Advances, 2015, 5, 17905-17914.	3.6	4
116	Enhancing the properties of perovskite quantum dot light emitting devices through grid structures formed by trioctylphosphine oxide. Journal of Materials Chemistry C, 2020, 8, 9861-9866.	5.5	4
117	Improved efficiency of hybrid solar cell based on thiolsâ€passivated CdS quantum dots and poly(3â€hexythiophene). Physica Status Solidi (A) Applications and Materials Science, 2012, 209, 1583-1587.	1.8	3
118	Interfacially Engineered Highâ€Speed Nonvolatile Memories Employing pâ€Type Nanoribbons. Advanced Materials Interfaces, 2014, 1, 1400130.	3.7	3
119	Carbon-wrapped four-component Na–Ni–Ti–Co oxides via sol–gel process for NIB anode material with superior cycling stability. Journal of Applied Electrochemistry, 2017, 47, 855-864.	2.9	3
120	Perovskite Lightâ€Emitting Diodes: Efficient CsPbBr <sub>3</sub> Perovskite Lightâ€Emitting Diodes Enabled by Synergetic Morphology Control (Advanced Optical Materials 4/2019). Advanced Optical Materials, 2019, 7, 1970014.	7.3	3
121	Batteries: Electrochemically Stable Sodium Metalâ€∓ellurium/Carbon Nanorods Batteries (Adv. Energy) Tj ETQq1 (	1 0,78431 19.5	4 ggBT /Ove
122	Full density graphite/copper-alloy matrix composite fabricated via hot powder forging for pantograph slide. Materials Research Express, 2021, 8, 066504.	1.6	3
123	Photodetectors: Fabrication of Ultrathin Bi2S3Nanosheets for High-Performance, Flexible, Visible-NIR Photodetectors (Small 24/2015). Small, 2015, 11, 2847-2847.	10.0	2
124	Converting electrical conductivity types in surface atomic-ligand exchanged PbS quantum dots via gate voltage tuning. Journal of Alloys and Compounds, 2017, 699, 866-873.	5.5	2
125	A Phosphine-Free Route to Size-Adjustable CdSe and CdSe/CdS Core–Shell Quantum Dots for White-Light-Emitting Diodes. Journal of Nanoscience and Nanotechnology, 2018, 18, 1864-1869.	0.9	2
126	Pulsed laser assisted synthesis of gadolinium carbide/carbon shell dots with enhanced magnetic resonance properties. Nanotechnology, 2019, 30, 105705.	2.6	2

YANG JIANG

#	Article	IF	CITATIONS
127	Bifunctional Interface Engineering by Oxidating Layered TiSe <sub>2</sub> for High-Performance CsPbBr <sub>3</sub> Solar Cells. ACS Applied Energy Materials, 0, , .	5.1	2
128	A NEW RED PHOSPHOR OF THE Mn ACTIVATED NON-STOICHIOMETRIC STRONTIUM ALUMINATE 3SrO•5Al2O3 FOR HIGH COLOR RENDERING WHITE LEDS. Functional Materials Letters, 2013, 06, 1350028.	<sup>3</sup> 1.2	1
129	Shape control of Ag nanostructures via a postsynthetic annealing treatment. CrystEngComm, 2014, 16, 7885.	2.6	1
130	Scale Synthesis of Environment Friendly CIZS/ZnS Core/Shell Quantum Dots for High Color Quality White LEDs. Nano, 2017, 12, 1750014.	1.0	1
131	Highly crystallized glass-ceramics from high content gold tailings <i>via</i> a one-step direct cooling method. RSC Advances, 2022, 12, 14175-14182.	3.6	1
132	Copper fiber reinforced needle-coke/carbon composite for pantograph slide and its current-carrying wear performance. Materials Research Express, 2022, 9, 055605.	1.6	1
133	Back Cover: Oneâ€pot synthesis of homogeneous CdSe <sub><i>x</i></sub> S <sub>1â^'<i>x</i></sub> alloyed quantum dots with tunable composition in a green Nâ€oleoylmorpholine solvent (Phys. Status) Tj ETQq1 I	1 <b>D</b> ø78431	.40rgBT /Ov€
134	Lithium Compounds: Reduced Local Symmetry in Lithium Compound Li <sub>2</sub> SrSiO <sub>4</sub> Distinguished by an Eu <sup>3+</sup> Spectroscopy Probe (Adv. Sci. 16/2019). Advanced Science, 2019, 6, 1970096.	11.2	0
135	Narrow-Bandgap Semiconductors of Perovskite Rare-Earth Orthoferrites (REFeO3). Current Chinese Science, 2021, 1, 438-452.	0.5	0
136	Synthesis of Eco-Friendly High PL Lifespan Manganese-Doped CulnZnS/ZnS QDs for White LED Applications. Journal of Nanoscience and Nanotechnology, 2020, 20, 6286-6294.	0.9	0